Dilational triangulated shells using pantographs

Broeren, F.G.J.; van de Sande, Werner; Van Der Wijk, V.; Herder, J. L.

DOI
10.1109/REMAR.2018.8449876

Publication date
2018

Document Version
Accepted author manuscript

Published in
2018 International Conference on Reconfigurable Mechanisms and Robots, ReMAR 2018 - Proceedings

Dilational Triangulated Shells Using Pantographs

F.G.J. Broeren[1,2]; W.W.P.J. van de Sande[1]; V. van der Wijk[1] and J.L. Herder[1]

Abstract— **Dilational structures are one degree of freedom structures able to change their size without changing their global shape. In this paper, we present a method to create dilational shells with arbitrary curvature. For this, we designed triangular tiles, which can be placed on a triangulation of the desired surface. We present the method and illustrate it with the example of a dilational octahedron. Using this regular polygon, we demonstrate that the whole structure has a single degree of freedom, and that the maximum obtainable scaling factor is directly linked to the range of motion of the individual triangular tiles.**

I. INTRODUCTION

Dilational structures expand in all directions when actuated, changing their size but keeping their global shape[1], [2]. These structures have been applied in many fields, for example architecture[3], space[4] and medicine[5]. A well-known example of a dilational structure is the Hoberman Sphere [6], [7]. This structure uses scissor-linkages to expand or contract radially when actuated. Dilational structures are often used for their ability to be compacted into a small volume and expanded on-site into a bigger, functional structure.

Recently, research into mechanical metamaterials has sprung renewed interest in dilational properties of structures, specifically for use as material structures with negative Poisson's ratios[8]. Dilation is obtained within this class of structures if the Poisson's ratio is -1.

Mechanical metamaterials are constructed out of a periodic array of unit cells; identical mechanical sub-units that make up the bulk of the structure. The material properties are governed by these unit cells, and therefore, the dimension of the metamaterial is equal to the dimension of the unit cell. Consequently, materials constructed out of 3D unit cells can not be used to form thin shells.

Alternatively, metamaterials constructed out of 2D unit cells are designed to be planar[9], [10]. These materials are made with planar periodicity in mind, which can not generally be fullfilled for arbitrarily curved surfaces.

Structures such as the Hoberman Sphere, which form a curved surface, rely on a mechanism that protrudes out of the surface when it is actuated, changing the effective thickness of the shell during motion.

In this paper, we present a method to create dilational shells with arbitrary curvature of which the mechanism stays locally in-plane throughout the range of motion, i.e. no parts of the mechanism protrude out of the shell. We propose to construct these shells from triangular tiles with an internal mechanism based on the (skew) pantograph linkage[11], [12], [13]. Each tile has a single, dilating degree of freedom and we will show how such tiles can be coupled with revolute pairs such that a dilating surface with a single degree of freedom is formed.

The mechanisms formed in this method fall into the category of general dilational polyhedra [14]. Our method stands out in this larger family of linkages because it can work for any polyhedral shape, without restrictions on regularity or convexity.

The dilational structures proposed in this paper form thin, hollow structures that have near-constant thickness throughout the range of motion, with no parts protruding into the enclosed volume. This makes our method suitable for applications where the dilational structure encloses a sensitive object, such as is, for example, the case in exoskeletons.

In the Methods section, we introduce the triangular tiles, show the conditions under which these are dilational, and present the necessary considerations for the coupling of these tiles. We then apply this method to the case of an octahedron. We show how the triangular tiles can be fitted on the triangular faces of the octahedron and determine the theoretical boundaries for its volume change. Finally, we investigate the feasibility and manufacturability of these structures by constructing the dilating octahedron and investigating the scaling properties of the structure under actuation.

We conclude the paper with a Discussion and Conclusion section, in which we discuss the usability and limitations of this technique for other cases than the octahedron presented here.

II. METHOD

A. Dilation of structures

Our goal is to obtain uniform scaling or dilation of any structure. Uniform scaling shrinks or enlarges a structure by a certain scaling factor. The resulting global structure is similar to the original in the geometric sense; the orientation is also preserved. Dilation is a special case of a homothetic transformation[15]:

$$A'B' = \lambda AB \tag{1}$$

A dilation transforms a line segment AB into a line $A'B'$ whose length is scaled by a factor λ. A dilation transforms all lines into parallel lines[16]. In addition, the lines joining the points with their transformed versions are concurrent in a point O, such that for a structure, consisting out of points A, B, C and D, we can write:

[1]Department of Precision and Microsystems Engineering, Delft University of Technology, 2628 CD Delft, the Netherlands
[2]Corresponding author, f.g.j.broeren@tudelft.nl

978-1-5386-6380-6/18/$31.00 ©2018 IEEE

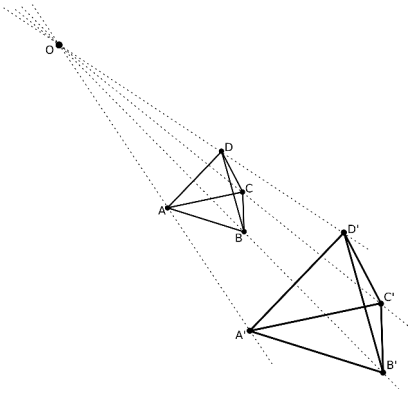

Fig. 1: Uniform scaling of a tetrahedron: all faces and edges remain similar and the orientations of the faces remain equal.

$$\begin{aligned}\overrightarrow{OA'} &= \lambda\overrightarrow{OA},\\ \overrightarrow{OB'} &= \lambda\overrightarrow{OB},\\ \overrightarrow{OC'} &= \lambda\overrightarrow{OC}, \text{ and}\\ \overrightarrow{OD'} &= \lambda\overrightarrow{OD},\end{aligned} \tag{2}$$

as is shown in fig. 1 for the example of a tetrahedron.

To create a dilational structure, eq. 2 must hold for any set of points in the structure. For practical purposes, we choose to approximate the desired structure by a triangulation. We choose subset of points on the surface which will follow eq. 2, and replace the rest of the structure with planar triangular tiles between the chosen points. The result is a polyhedron that is an approximation of the structure and this approximation becomes more accurate when more points on the original surface are considered. Taking point O to be the origin, we can write for a chosen set of points V

$$v' : \lambda v \quad \forall v \in V. \tag{3}$$

All edges and faces of the resulting polyhedra must be similar and homothetic. Therefore, the vector normal to any face can not change under dilation.

B. Triangular tiles

To construct a dilating structure from our triangulated surface, we propose to use triangular tiles based on Sylvester's plagiograph or skew pantograph [11], [17]. This mechanism is drawn in fig. 2. It is a reduced case of the general pantograph and consists of two similar triangular bodies and two links. They construct a planar parallelogram linkage with one degree of freedom. For our application, we choose the rigid triangles to have the same size.

This mechanism has the following properties that are useful for our application:

- it has only one degree of freedom
- it is planar
- three points of the mechanism span a triangle that remains similar while subject to motion (this property will be proven in the next subsection)

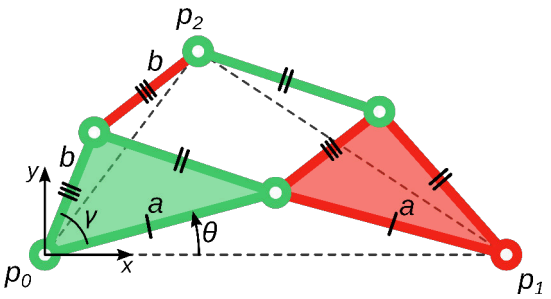

Fig. 2: Sylvester's plagiograph, the mechanism is defined by the lengths, a, b and the angle γ. Revolute joints are shown as circles and equal sides by hatches. The dotted line indicates the triangle spanned by this mechanism, which stays similar when the angle θ changes.

At each face of the triangulated surface, one pantograph mechanism will be placed such that points p_0, p_1, p_2 coincide with the vertices of the triangular face. At each edge, two neighboring tiles meet and share two vertices. At these vertices, the links of the two pantograph mechanisms are joined by revolute pairs, such that the relative orientation of the two pantographs is fixed. Effectively this creates a two-sided sarrus linkage[18] coupling the motion of two adjacent faces, creating a 1-DOF structure.

C. Similarity proof

In order for a polyhedron constructed from these triangular tiles to be dilational, each of the triangular tiles should undergo a dilation when actuated. We take the triangle spanned by the pantograph mechanism to be spanned by p_0, p_1, p_2 and write their positions as

$$\begin{aligned}p_0 &= \{0 \quad 0\}^T\\ p_1 &= \{2a \quad 0\}^T\\ p_2 &= 2b\{\cos(-\gamma) \quad \sin(\gamma)\}^T\end{aligned} \tag{4}$$

When actuated, the rigid triangles will rotate with respect to each other. We take the point p_0 to be fixed, and constrain p_1 to lie on the x-axis. Then, when the left rigid triangle rotates by an angle θ around p_0, the right rigid triangle rotates by an angle $-\theta$ around p_1. This transforms the points p_1, p_2 in to the points p_1', p_2':

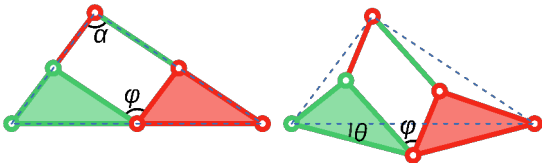

Fig. 3: Motion of the triangular tile as a function of the rotation θ; in all poses the opposite angles of the parallelogram will be equal

$$\begin{aligned} p_1' &= \{\cos(\theta)a+\cos(-\theta)a \quad \sin(\theta)a+\sin(-\theta)a\}^T \\ &= \{\cos(\theta)2a \quad 0\}^T \\ &= \cos(\theta)\{2a \quad 0\}^T \\ &= \cos(\theta)p1 \end{aligned} \tag{5}$$

$$\begin{aligned} p_2' &= \begin{Bmatrix} \cos(\gamma+\theta)b+\cos(\gamma-\theta)b \\ \sin(\gamma+\theta)b+\sin(\gamma-\theta)b \end{Bmatrix} \\ &= 2b\begin{Bmatrix} \cos(\gamma)\cos(\theta) \\ \sin(\gamma)\cos(\theta) \end{Bmatrix} \\ &= 2b\cos(\theta)\begin{Bmatrix} \cos(\gamma) \\ \sin(\gamma) \end{Bmatrix} \\ &= \cos(\theta)p_2. \end{aligned} \tag{6}$$

In the above, the angle sum and difference trigonometric identities are used to simplify the expressions. The points p_1 and p_2 are scaled by the same factor $\lambda = \cos(\theta)$ and the point p_0 was assumed to be fixed. Therefore, the whole triangle scales isotropically with the factor λ and $\triangle p_0p_1p_2 \sim \triangle p_0p_1'p_2'$.

This way, we have proven that, when the pantograph mechanism is actuated, the triangle spanned by the points p_0, p_1', p_2' stays similar to the original triangle p_0, p_1, p_2 and that the triangle is scaled by a factor $\lambda = \cos(\theta)$.

D. Range of Motion

All parts of the triangular tile move in the same plane; consequently, the tile has limits in its range of motion at the points where its geometry will intersect. This will happen when the area of the parallelogram becomes zero. This equates to two opposite angles of the parallelogram becoming zero. There are two possibilities for this: when the angle ϕ in fig. 3 becomes zero, or when it becomes equal to π.

We call the top angle of the spanned triangle α. When the area of this spanned triangle is maximal, $\phi = \alpha$. This angle can be deduced using the dimensions of the triangle and the cosine law.

As one of the links rotates clockwise, the other turns counter-clockwise. The included angle between the two links in motion is as follows:

$$\phi(\theta) = \alpha + 2\theta. \tag{7}$$

One limit of motion is found for $\theta_1 = -\frac{\alpha}{2}$. At this point, de angle ϕ becomes zero.

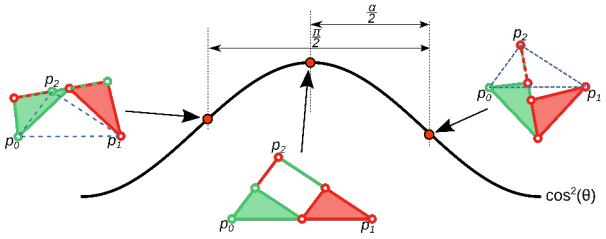

Fig. 4: Scaling of the triangular tile as a function of the rotation θ, the range of motion is indicated by the dots, the corresponding branch of motion is also illustrated

The other limit of the motion is found for $\phi = \pi$, in this case, we have $\theta_2 = \frac{\pi-\alpha}{2}$.

The range of motion of the rotation θ is defined as the difference of the limits of motion.

$$ROM = \theta_2 - \theta_1 = \frac{\pi-\alpha}{2} + \frac{\alpha}{2} = \frac{\pi}{2} \tag{8}$$

The movement and the scaling of the triangular tile is illustrated in fig. 4.

All triangular tiles share the same degree of freedom; therefore they share the same scaling parameter $\lambda^2 = \cos^2(\theta)$. The range of motion of each triangle is $\frac{\pi}{2}$; this would indicate a maximum scaling of:

$$\lambda^2(\pm\frac{\pi}{2}) = \cos^2(\pm\frac{\pi}{2}) = 0. \tag{9}$$

This solution effectively sacrifices one branch of motion to maximise the motion in the other. This is not feasible since the top angle of the spanned triangle would then become π or zero; which is a triangle without area. Another solution is to divide the range of motion over the branches evenly: $\theta = \pm\frac{\pi}{4}$. In this case the maximum area change of the triangle is as follows:

$$\lambda^2(\pm\frac{\pi}{4}) = \cos^2(\pm\frac{\pi}{4}) = \frac{1}{2}. \tag{10}$$

This has the effect that the top angle α is a right angle, which can be deduced from equation 7 . If every polygon in the polyhedron is a right triangle, maximum volume change of the polyhedron is as follows:

$$\lambda^3 = \sqrt{\frac{1}{2}}^3 = \frac{1}{2\sqrt{2}} \approx 0.354. \tag{11}$$

This scaling is irrespective of the branches of motion of the triangular tiles. In polyhedra of non-similar triangles the scaling of the polyhedron is dependent on the branches of the tiles and the corresponding scaling parameter. The degree of freedom is shared by all tiles. Therefore the polyhedron also has two branches. In each of the branches, the scaling of the polyhedron will be limited by the tile (or set of tiles) that reaches its limit first.

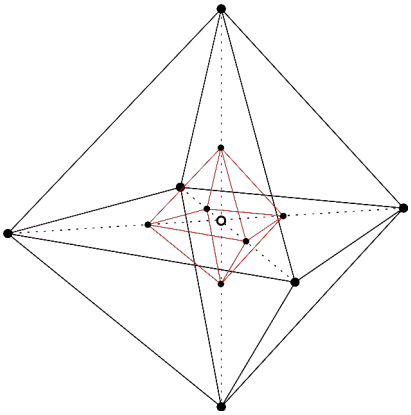

Fig. 5: Uniform scaling of an octahedron with dilation center indicated in the center of the polyhedron

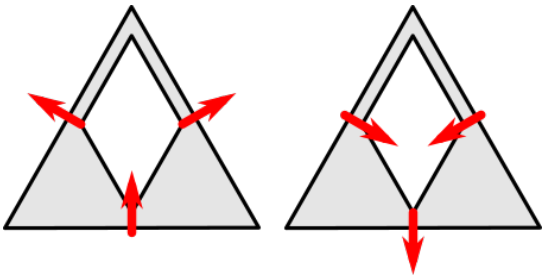

Fig. 6: The two possible motions of a triangular unit cell. The red arrows indicate the directions of the motion at three hinge positions.

III. CASE: OCTAHEDRON

We apply the method to a simple polyhedron: a regular octahedron. This is a Platonic solid made up out of 8 equilateral triangles. Four faces meet at every vertex of which there are six. The mid-plane is a square. The center of this square will be the dilation center of the mechanism. It can be seen from fig. 5 that all vectors from the dilation center to all vertices scale uniformly. Every edge and face remains similar; consequently all faces can be replaced by triangular tiles to enable uniform scaling.

A. Placement of the tiles on an octahedron

At the base of the triangular tiles lies a four-bar linkage. As a result, two sides of the triangular tile will move in an opposite direction of the third one under actuation (fig. 6). All equilateral triangular tiles have the same range of motion, parametrized by θ: $\theta = [-\pi/3, \pi/6]$; this can be seen from the shape of the four-bar linkage at $\theta = 0$.

When joining the triangles at their shared corners, the motion directions of the sides of the triangular tiles need to be considered to avoid collisions between the tiles.

For the octahedron, we chose the configuration shown in fig. 7. This has been determined to be a collision-free orientation by drawing the arrows onto the tiles by hand. Note that, in this figure, all arrows can be reversed without breaking the tiling pattern. This reflects the fact that there are two branches of motion for this mechanism.

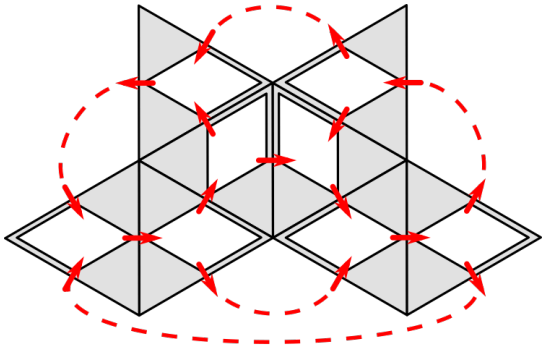

Fig. 7: The orientation of the triangular tiles on the net of the octahedron.

B. Dilational properties of the octahedron

When the above described orientation of the triangular tiles is used, each of the tiles has the same mobility, parametrized by θ: $\theta = [-\pi/6, \pi/6]$. This is due to the fact that the described orientation contains both branches of motion of the triangular tile; this limits the motion of the mechanism. All triangles have the same dimensions and are equilateral, therefore we can express the side lengths as

$$L = 2a\cos(\theta), \tag{12}$$

where a is half the side length of the triangles at $\theta = 0$. This means that the side lengths of the triangles are at most $L = 2a$, for $\theta = 0$, and at a minimum at $\theta = \pm\pi/6$, where $L = \sqrt{3}a$. Using this, we can determine the ratio of volume change:

$$\begin{aligned} \frac{V(\theta = \pm\frac{pi}{6})}{V(\theta = 0} &= \lambda^3 \\ &= \cos^3(\pm\frac{\pi}{6}) \\ &= \frac{9}{8\sqrt{3}} \approx 0.65 \end{aligned} \tag{13}$$

So, under perfect conditions, the octahedron could undergo a volume change of 35% and the scaling parameter would be $\lambda = \frac{\sqrt{3}}{2} \approx 0.866$.

C. Experimental analysis

We constructed the dilational octahedron by laser-cutting triangles and bars from 5mm PMMA sheet and assembling them onto 3D printed connectors with M6 bolts. The tiles were placed according to the orientation shown in fig. 7.

The octahedral structure was actuated manually and the distance between two opposing vertices was measured in both the fully extended and the fully compacted state (see fig. 8). Dividing the height in the compacted state by the height of the octahedron in the extended state gave us a scaling parameter $\lambda = 0.937$, which is substantially higher compared to the ideal case.

The difference in scaling factor can be explained when we look at a single unit cell, as shown in fig. 9. Because of the thickness of the bars, the range of motion of the mechanism

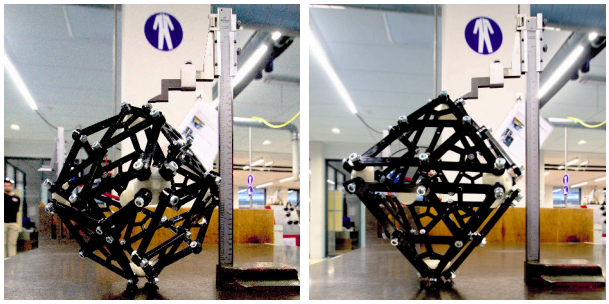

(a) $H = 253mm$ (b) $H = 270mm$

Fig. 8: Measurements of the distance between two opposing vertices of the octahedral structure. The measured heights are given in the subcaptions.

is smaller than in the ideal case. We measured the range of motion in ϕ to be

$$ROM_{\phi} = [13^{\circ}, 102^{\circ}] \tag{14}$$

corresponding to

$$ROM_{\theta} = [23.5^{\circ}, -21^{\circ}]. \tag{15}$$

For this range of motion, we can calculate the scaling factor:

$$\lambda(23.5^{\circ}) = \cos(23.5^{\circ}) \approx 0.917 \tag{16}$$

$$\lambda(-21.0^{\circ}) = \cos(-21^{\circ}) \approx 0.934 \tag{17}$$

These scaling factors are much closer to the scaling factor we measured from the height of the octahedron, indicating that the thickness of the bars is indeed the predominant factor in limiting the range of motion of the dilating octahedron.

Because the octahedral linkage was constructed in its expanded state, all of the linkages on the faces were in their singular position. When actuating the octahedron, we had to take special care to make every face follow the correct motion branch for the tiling pattern. We solved this problem by attaching rubber bands to the links of the mechanism, making the lowest energy configuration non-singular and following the desired motion branch. This solution is shown in fig. 10.

IV. DISCUSSION

As mentioned in the Methods section, our goal was to obtain uniform scaling, or dilation, of any shell-like structure. In the Experimental part of this paper, however, we have only shown that the method works for a relatively simple polyhedron. Although this polyhedron is regular and has all equal and equilaterial triangular faces, the way in which the octahedron was constructed contained all the steps necessary to construct a dilating structure from an arbitrarily curved surface using our methodology. In this section we would like to highlight how the steps in the construction of the octahedron relate to the construction of a general dilational surface.

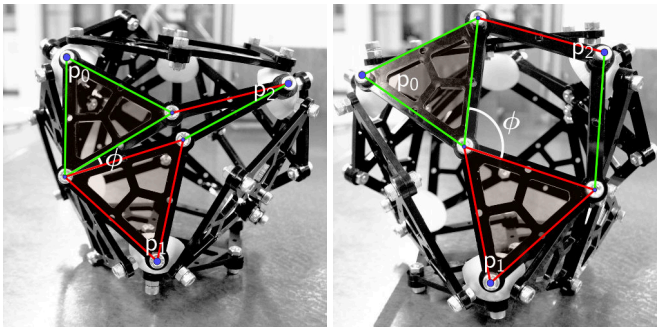

(a) $\phi = 13^{\circ}$ (b) $\phi = 102^{\circ}$

Fig. 9: Two faces of the octahedron in the compacted state. The lines drawn on top were used to estimate the angle ϕ in this configuration, the labels p_0, p_1, p_2 refer to the points drawn in fig. 2

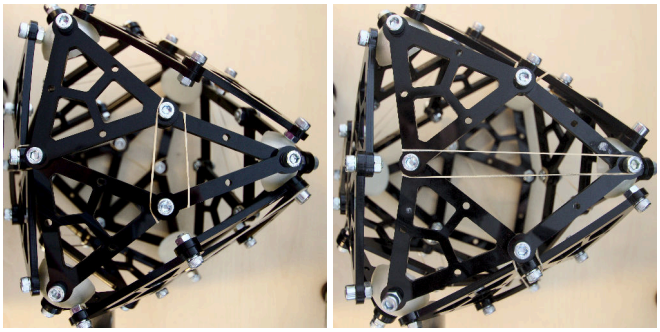

(a) (b)

Fig. 10: Two faces of the octahedron with rubber bands applied to change the lowest-energy configuration to a non-singular one.

First, for an arbitrary curved surface, the surface needs to be triangulated. In the case of the octahedron this was not necessary, since the surface already existed out of triangles. Alternatively, the octahedron could be viewed as a, very coarse, triangulation of a sphere.

Secondly, a possible orientation of the triangular tiles on the surface needs to be found that preserves mobility using the method shown in fig. 7. Although the difficulty of this step will increase with the size of the net, the method of drawing in the arrows to find a suitable orientation still applies.

Lastly, the triangular tiles are designed to fit the faces of the triangulation and are connected rigidly to each other. In the general case, this would involve constructing each face individually and keeping track of the correct placement of all the tiles. For the octahedron, only one equilateral triangular face had to be designed, since all faces are equal. The only thing to take into account is the orientation of the tiles.

In the Methods section, we showed that the skew pantograph can can be constructed for any general triangle, so the construction of the triangular tiles is possible for any triangulation. However, if the triangulation contains triangles with very sharp corners, the range of motion of the entire

mechanism will be small. This effect needs to be taken into account when triangulating the desired surface.

In the experimental section, we also noted that, although a fitting orientation of the triangular tiles was used, it was still possible for individual faces to follow a colliding branch of motion due to a singularity of the mechanism in the expanded state. This caused collisions between parts of the mechanism, thereby severely impacting the range of motion. We solved this by the addition of potential energy in the form of rubber bands, shifting the lowest energy state to a non-singular one. For larger, more complex structures, a different method of achieving this, involving less manual labour, will be required.

V. CONCLUSION

In this paper, we have shown a method to create thin, dilational structures with an arbitrarily curved surface. This method consists out of triangulating the surface, and replacing the triangular faces with a one degree of freedom mechanism based on the skew pantograph. These mechanisms are then coupled at the corners of the triangular faces such that a single degree of freedom is shared by all triangular mechanisms.

We have shown that the permitted motion of the skew pantograph dilates the triangle described by its three corners, and that the dilating properties of the individual triangles translates into an overall dilation of the structure when the triangles are coupled by revolute pairs at their corners. To illustrate this method, we have constructed a dilational octahedron, and highlighted the most prominent pitfalls and considerations in doing so. We constructed the dilational octahedron from laser-cut PMMA and 3D printed connectors and experimentally determined its scaling factor to be 0.937.

This work presents a first step towards the creation of dilating shell-like structures with arbitrary curvature. Many applications exist for such structures, from deployable sculptures, that can be shrunk or enlarged to fit a space or for transportation purposes, to exoskeletons, where the auxetic properties of the shell can help in better fitting around the body.

REFERENCES

[1] G. W. Milton, "New examples of three-dimensional dilational materials," *Phys. status solidi*, vol. 252, no. 7, pp. 1426–1430, jul 2015.

[2] ——, "Composite materials with poisson's ratios close to 1," *J. Mech. Phys. Solids*, vol. 40, no. 5, pp. 1105–1137, jul 1992.

[3] E. Rivas Adrover, *Deployable Structures*. London: Laurence King Publishing, 2015.

[4] R. J. Lang, S. Magleby, and L. Howell, "Single Degree-of-Freedom Rigidly Foldable Cut Origami Flashers," *J. Mech. Robot.*, vol. 8, no. 3, p. 031005, mar 2016.

[5] M. N. Ali, J. J. C. Busfield, and I. U. Rehman, "Auxetic oesophageal stents: structure and mechanical properties," *J. Mater. Sci. Mater. Med.*, vol. 25, no. 2, pp. 527–553, feb 2014.

[6] C. Hoberman, "Radial expansion/retraction truss structures," US Patent US5 024 031, 06 18, 1991.

[7] ——, "Reversibly expandable doubly-curved truss structure," US Patent US4 942 700, 07 24, 1990.

[8] K. E. Evans and A. Alderson, "Auxetic Materials: Functional Materials and Structures from Lateral Thinking!" *Adv. Mater.*, vol. 12, no. 9, pp. 617–628, may 2000.

[9] J. N. Grima, A. Alderson, and K. E. Evans, "Auxetic behaviour from rotating rigid units," *Phys. status solidi*, vol. 242, no. 3, pp. 561–575, mar 2005.

[10] J. T. B. Overvelde, S. Shan, and K. Bertoldi, "Compaction Through Buckling in 2D Periodic, Soft and Porous Structures: Effect of Pore Shape," *Adv. Mater.*, vol. 24, no. 17, pp. 2337–2342, may 2012.

[11] J. J. Sylvester, "On the plagiograph aliter the skew pantigraph," *Nature*, vol. 12, p. 168, jul 1875.

[12] E. Dijksman, *Motion geometry of mechanisms*. Cambridge, UK: Cambridge University Press, 1976.

[13] G. Kiper, E. Söylemez, and A. Ö. Kiisel, "A family of deployable polygons and polyhedra," *Mech. Mach. Theory*, vol. 43, no. 5, pp. 627–640, 2008.

[14] G. Kiper and E. Söylemez, "Polyhedral linkages obtained as assemblies of planar link groups," *Frontiers of Mechanical Engineering*, vol. 8, no. 1, pp. 3–9, Mar 2013. [Online]. Available: https://doi.org/10.1007/s11465-013-0363-6

[15] B. Meserve, *Fundamental concepts of geometry*. Cambridge (Mass.): Addison-Wesley, 1955.

[16] H. S. M. Coxeter and S. L. Greitzer, *Geometry revisited*, ser. New Mathematical Library. Mathematical Association of America, 1967.

[17] J. J. Sylvester, "History of the plagiograph," *Nature*, vol. 12, pp. 214–216, jul 1875.

[18] P. Sarrus, "Note sur la transformation des mouvements rectilignes alternatifs, en mouvements circulaires, et reciproquement," *Comptes Rendus*, vol. 36, p. 1036, 1853.